Supporting Information

Amyloid-Like Assembly Converting Commercial Proteins to Water-Insoluble Adsorbents with Ultrahigh Adsorption Capacity and Ultrafast Adsorption Rate for Uranium Extraction

Hao Ye [a], Ming-Bang Wu [a]*, Lu-Lin Ma [a], Shi-Cheng Liu [a], Yu Zhong [a], Juming Yao[a,b]

[a]*School of Materials Science and Engineering, Zhejiang Sci-Tech University, 928 Second Avenue, Xiasha Higher Education Park, Hangzhou 310018, China Hangzhou 310018, China*

[b]*School of Materials Science and Chemical Engineering, Ningbo University, 818 Fenghua Road, Ningbo 315211, China*

E-mails: wumingbang@zstu.edu.cn (M.-B. Wu),

Molecular dynamics simulations:

Structure optimization of BSA: All-atom crystal structure of BSA analyzed by Bujacz et al. was obtained from RCSB Protein Data Bank [S1-2]. The coordinates of co-crystallized water molecules were deleted before simulations and the disulfide bonds of BSA were broken to adapt to the role of TCEP. First, BSA was solvated in a rectangular box ($160 \times 81 \times 108$ Å^3) using the SPC/E water model [S3] and neutralized by sodium cations. The conjugate gradient method [S4-5] was used to pre-equalize the system for eliminating the excessive stress in initial structures. After energy minimization, a 300 ps position-restrained NPT process was performed to relax the solvent around the protein at 298 K, during which the temperature and pressure coupling were performed using a v-rescale thermostat [S6] and Berendsen barostat [S7]. A 200 ns production simulation was then performed under NPT ensemble with Parrinello-Rahman barostat [S8].

Simulated ions adsorption: BSA and counterions were extracted from the as-equilibrated box and placed in the center of an empty rectangular box ($200 \times 100 \times 150$ Å^3). Then 38 Na^+, 70 UO_2^{2+}, 70 Fe^{3+}, 70 Mg^{2+}, 70 Cu^{2+}, 70 Co^{2+}, 70 Zn^{2+}, 140 NO_3^-, 808 Cl^-, and 40000 water molecules were randomly placed in the box using Packmol program [S9] for providing homogeneous electrolyte solution. The parameters of energy minimization, position-restrained simulation, and production simulation are the same as described above.

During simulations, three-dimensional periodic boundary conditions (PBC) were used to avoid the influence of the box boundary during simulations. The cut-off distance of non-bonded interactions is 13 Å and the long-range electrostatic interactions were calculated by the particle-mesh Ewald (PME) method [S10]. All simulations were based on Amber99sb-ildn force field [S11] and carried out by using the GROMACS 2018.6 software package [S12]. Parameters of UO_2^{2+} and NO_3^- were taken from Shenoy et al.

[S13], while other metal cations and anions were based on Merz's parameters [S14-16]. All visualization structures are provided by VMD 1.9.3 software [S17]. Radial distribution functions (RDF) $g(r)_{A-B}$ defined by equation S1:

$$g(r)_{A-B} = \frac{1}{\langle \rho_B \rangle} \frac{1}{N_A} \sum_{i=1}^{N_A} \sum_{j=1}^{N_B} \frac{\delta(r_{ij} - r)}{4\pi r^2}$$

was utilized to calculate the coordination number of UO_2^{2+}, with $\langle \rho_B \rangle$ the particle density of type B averaged over all spheres around particles A. Notably, RDF calculated in this work is between the center of mass of UO_2^{2+} (B in the equation) and van der Waals surface of BSA (A in equation).

Table S1. Comparison of adsorption performances with other state-of-the-art adsorbents.

Adsorbent	Adsorption capacity (mg/g)	Equilibrium time	Conditions	Ref.
BSA-TCEP	1064	2 h	V = 2 L, m = 5 mg, FR = 1 L/h	This work
PIDO NF	951	550 min	V = 5 L, m = 15 mg, FR = 5 L/min	[18]
MS@PIDO/Alg	539.19	24 h	V = 5 L, m = 60 mg, FR = 5 L/min	[19]
AO-HNTs	295.66	13 h	V = 1 L, m = 10 mg, FR = 1 L/h, T = 25 ℃, pH = 8	[20]
SSUP fiber	12.51	30 min	V = 30 mL, m = 10 mg	[21]
PAO hydrogel	718	600 h	V = 1 L, m = 10 mg	[22]
CP-PAO	350	160 h	V = 2 L, m = 10 mg	[23]
PPA@MISS-PAF-1	307.3	60 min		[24]
SMON-PAO fibers	1158.16	30 h	V = 5 L, m = 10 mg	[25]
UiO-66-3C4N	200	8 h	V = 1 L, m = 5 mg, pH = 8	[26]
H-ABP fiber	302	24 h	V = 1 L, m = 20 mg, pH = 8	[27]
UiO-66	340	14 h	V = 1 L, m = 10 mg, pH = 6	[28]
Zn^{2+}/PAO	664	36 h	V = 2 L, m = 10 mg	[29]
RGO/PDA/oxime	605	6 h	V = 500 mL, m = 5 mg, T = 25 ℃, pH = 5	[30]

V is the volume of the solution; m is the mass of the adsorbents; FR is flow rate; T is the temperature.

Table S2. Parameters of Pseudo-first-order and Pseudo-second-order adsorption kinetics for BSA-based adsorbents.

Concentration	Pseudo-second-order model			Pseudo-first-order model		
	R^2	q_e	k_2 (g/mg/min)	R^2	q_e	k_1 (min^{-1})
1 ppm	0.99509	314.47	7.2×10^{-4}	0.92283	310.77	0.065
4 ppm	0.99975	671.14	4.68×10^{-4}	0.90125	608.94	0.4521
8 ppm	0.99928	1074.61	1.18×10^{-4}	0.84129	907.27	0.3112
16 ppm	0.98949	2036.37	1.25×10^{-5}	0.9385	1727	0.0195
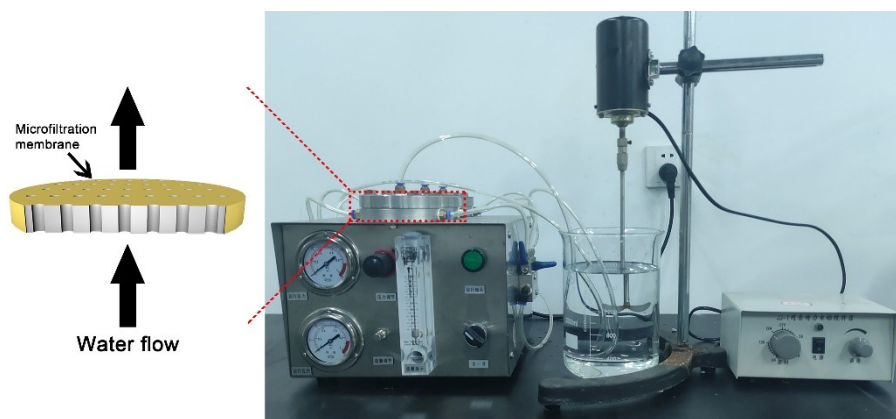
Fig. S1 Self-made flow system for testing adsorption performance.
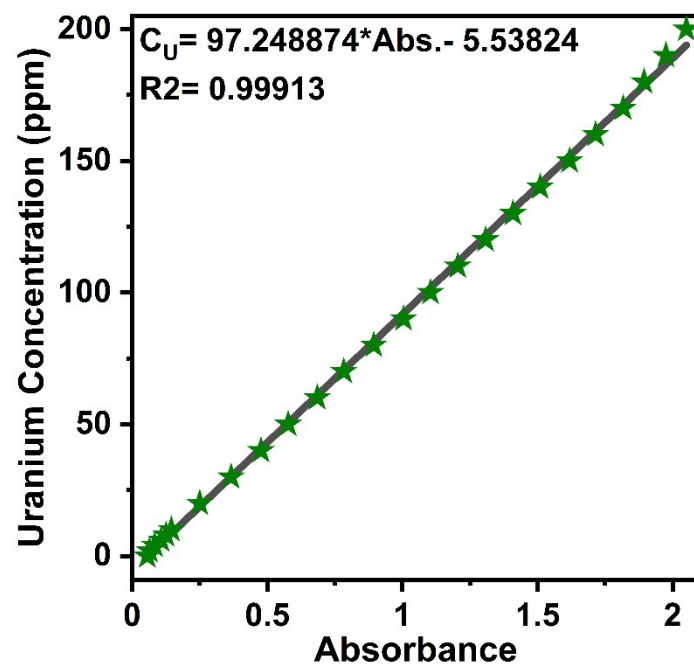
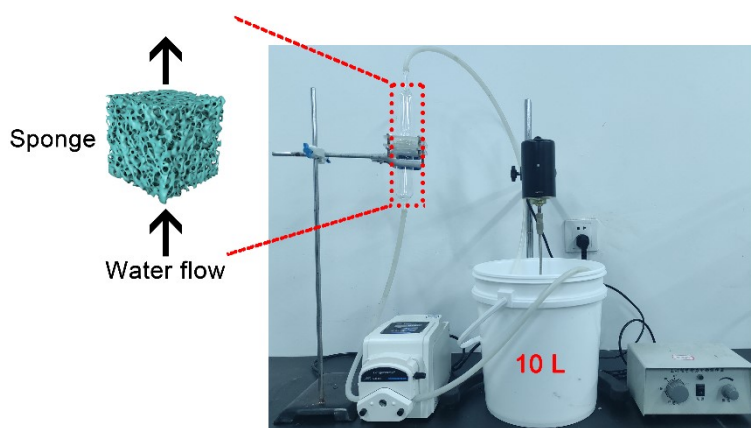**Fig. S2** The curvilinear regression between uranium concentration and absorbance.

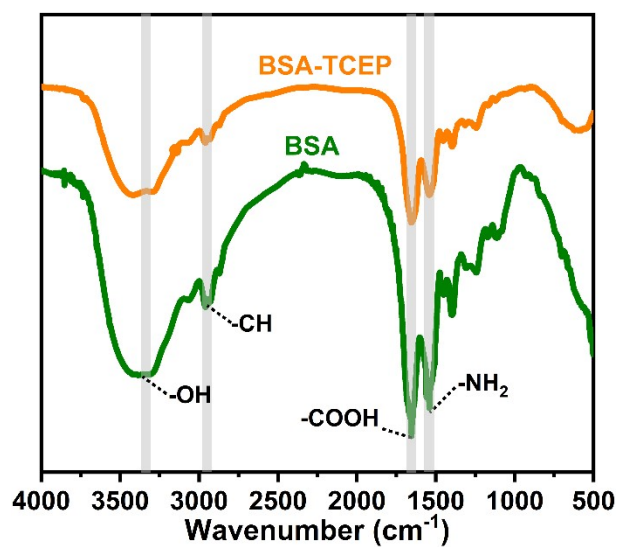**Fig. S3** Self-made circulating water flow system for dynamic adsorption.

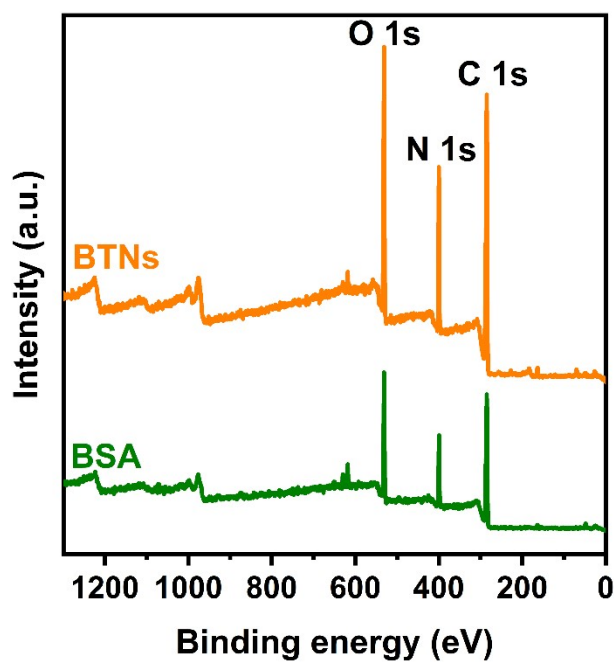**Fig. S4** FT-IR spectra of pristine BSA and BSA-based adsorbents.

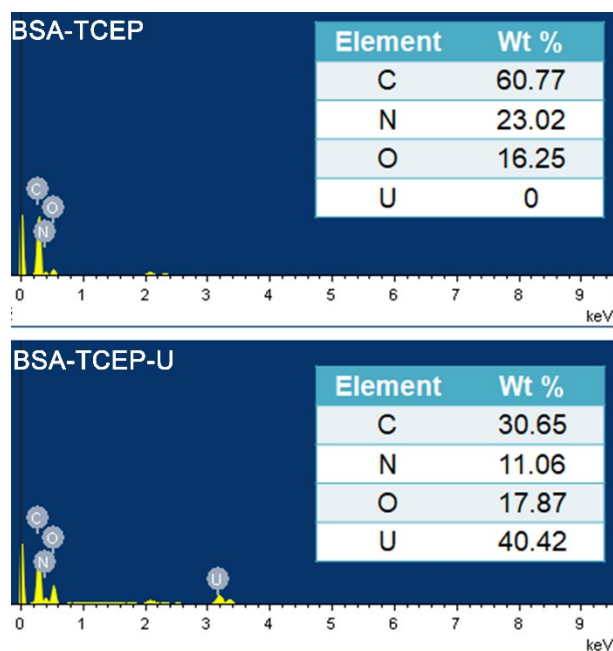**Fig. S5** XPS spectra of pristine BSA and BSA-based adsorbents.

Element	Wt %
C	60.77
N	23.02
O	16.25
U	0

BSA-TCEP

Element	Wt %
C	30.65
N	11.06
O	17.87
U	40.42

BSA-TCEP-U

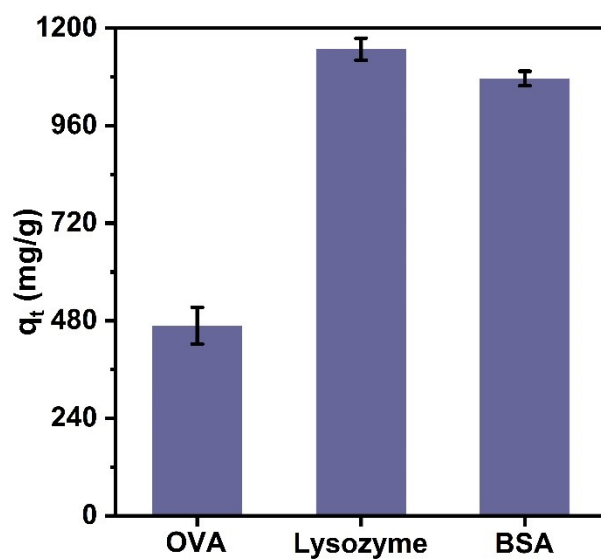**Fig. S6** EDS results of the adsorbents before and after adsorption.

Fig. S7 Adsorption capacity the protein-based adsorbents prepared by different proteins. The initial concentration of uranium is 8 ppm.
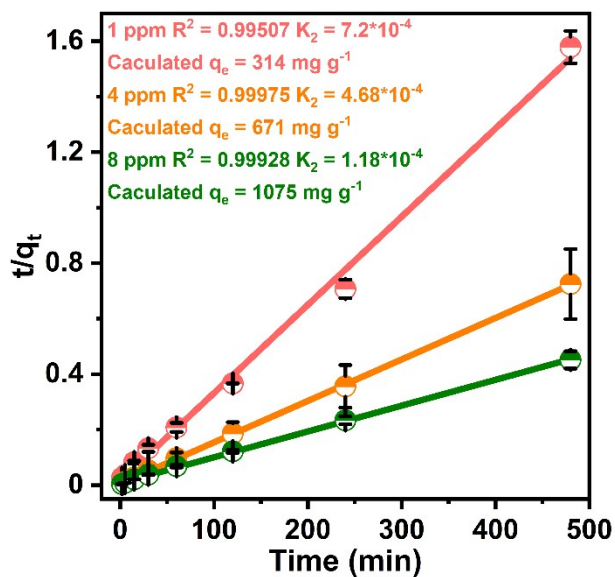
Fig. S8 Plots of t/q_t as a function of reaction time, showing the reactions followed by pseudo-second-order kinetic model.
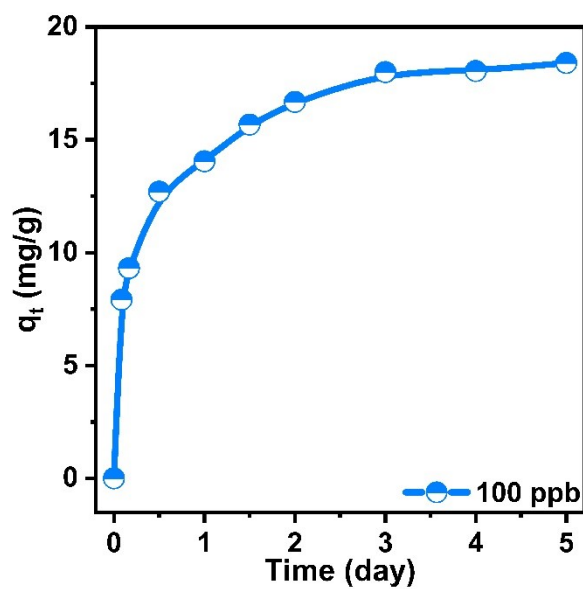

Fig. S9 The kinetics of uranium adsorption with an initial concentration of 100 ppb.
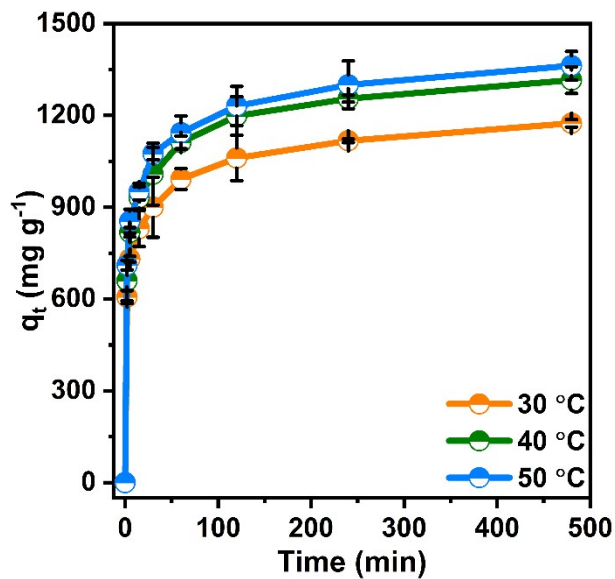
Fig. S10 Adsorption capacity of the adsorbents at different temperatures. The initial concentration of uranium is 8 ppm.
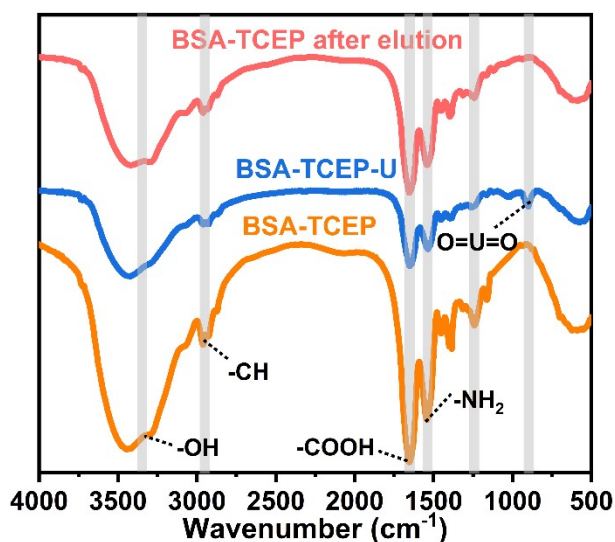

Fig. S11 FT-IR spectra of the adsorbents before adsorption, after adsorption and after desorption, respectively.
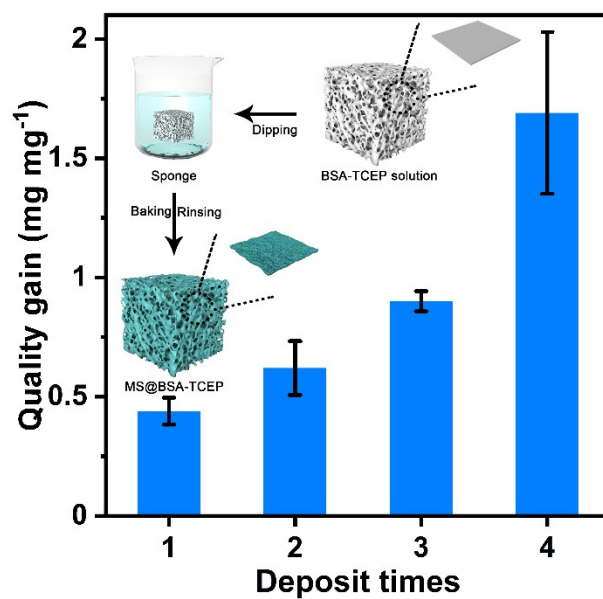
Fig. S12 Mass changes of modified sponges with different deposition times.
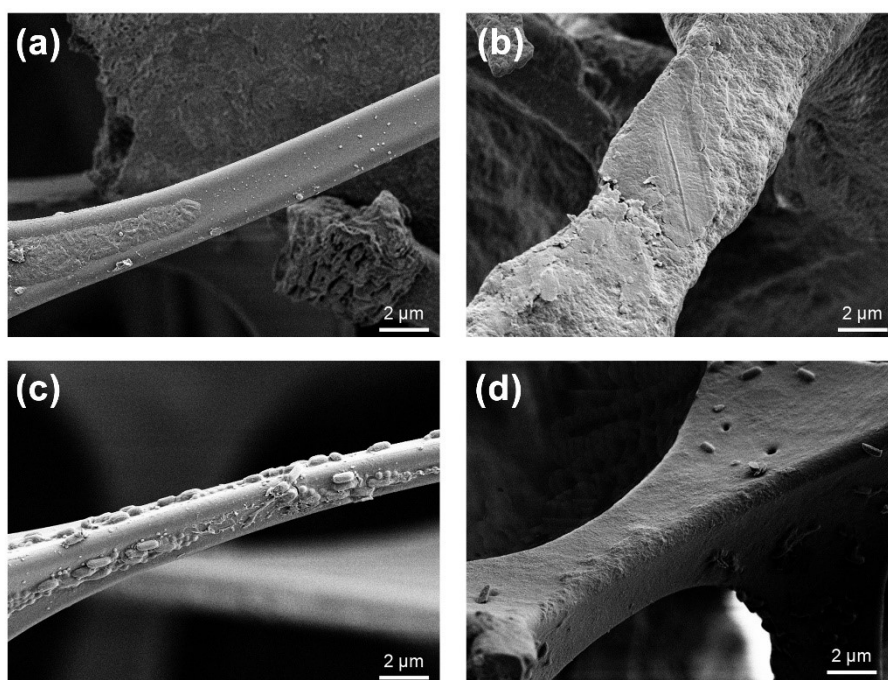

Fig. S13 SEM images of MS (a) without and (a) with BSA coatings after contacting with *Escherichia coli*, respectively. SEM images of MS (c) without and (d) with BSA coatings after contacting with *Staphylococcus aureus*, respectively.

References

[S1] A. Bujacz, Structures of bovine, equine and leporine serum albumin, Acta Crystallographica Section D, 68 (2012) 1278-1289.

[S2] B.G. Bujacz A., Crystal Structure of Bovine Serum Albumin, doi: 10.2210/pdb4F5S/pdb, (2012).

[S3] H.J.C. Berendsen, J.R. Grigera, T.P. Straatsma, The missing term in effective pair potentials, The Journal of Physical Chemistry, 91 (1987) 6269-6271.

[S4] K. Zimmermann, ORAL: All purpose molecular mechanics simulator and energy minimizer, 12 (1991) 310-319.

[S5] M.C. Payne, M.P. Teter, D.C. Allan, T.A. Arias, J.D. Joannopoulos, Iterative minimization techniques for ab initio total-energy calculations: molecular dynamics and conjugate gradients, Rev. Mod. Phys., 64 (1992) 1045-1097.

[S6] G. Bussi, D. Donadio, M. Parrinello, Canonical sampling through velocity rescaling, J. Chem. Phys., 126 (2007) 014101.

[S7] H.J.C. Berendsen, J.P.M. Postma, W.F. van Gunsteren, A. DiNola, J.R. Haak, Molecular dynamics with coupling to an external bath, J. Chem. Phys., 81 (1984) 3684-3690.

[S8] M. Parrinello, A. Rahman, Polymorphic transitions in single crystals: A new molecular dynamics method, J. Appl. Phys., 52 (1981) 7182-7190.

[S9] L. Martínez, R. Andrade, E.G. Birgin, J.M. Martínez, PACKMOL: A package for building initial configurations for molecular dynamics simulations, J. Comput. Chem., 30 (2009) 2157-2164.

[S10] T. Darden, D. York, L. Pedersen, Particle mesh Ewald: An N·log(N) method for Ewald sums in large systems, J. Chem. Phys., 98 (1993) 10089-10092.

[S11] K. Lindorff-Larsen, S. Piana, K. Palmo, P. Maragakis, J.L. Klepeis, R.O. Dror, D.E. Shaw, Improved side-chain torsion potentials for the Amber ff99SB protein force field, Proteins: Struct., Funct., Bioinf., 78 (2010) 1950-1958.

[S12] M.J. Abraham, T. Murtola, R. Schulz, S. Páll, J.C. Smith, B. Hess, E. Lindahl, GROMACS: High performance molecular simulations through multi-level parallelism from laptops to supercomputers, SoftwareX, 1-2 (2015) 19-25.

[S13] P. Sahu, S.M. Ali, K.T. Shenoy, Passage of TBP–uranyl complexes from aqueous–organic interface to the organic phase: insights from molecular dynamics simulation, Phys. Chem. Chem. Phys., 18 (2016) 23769-23784.

[S14] P. Li, L.F. Song, K.M. Merz, Systematic Parameterization of Monovalent Ions Employing the Nonbonded Model, J. Chem. Theory Comput., 11 (2015) 1645-1657.

[S15] P. Li, B.P. Roberts, D.K. Chakravorty, K.M. Merz, Rational Design of Particle Mesh Ewald Compatible Lennard-Jones Parameters for +2 Metal Cations in Explicit Solvent, J. Chem. Theory Comput., 9 (2013) 2733-2748.

[S16] P. Li, L.F. Song, K.M. Merz, Parameterization of Highly Charged Metal Ions Using the 12-6-4 LJ-Type Nonbonded Model in Explicit Water, J. Phys. Chem. B, 119 (2015) 883-895.

[S17] W. Humphrey, A. Dalke, K. Schulten, VMD: Visual molecular dynamics, J. Mol. Graph., 14 (1996) 33-38.

[S18] D. Wang, J. Song, J. Wen, Y. Yuan, Z. Liu, S. Lin, H. Wang, H. Wang, S. Zhao, X. Zhao, M. Fang, M. Lei, B. Li, N. Wang, X. Wang and H. Wu, *Advanced Energy Materials*, 2018, **8**, 1802607.

[S19] D. Wang, J. Song, S. Lin, J. Wen, C. Ma, Y. Yuan, M. Lei, X. Wang, N. Wang and H. Wu, *Advanced Functional Materials*, 2019, **29**, 1901009.

[S20] S. Zhao, Y. Yuan, Q. Yu, B. Niu, J. Liao, Z. Guo and N. Wang, *Angewandte Chemie International Edition*, 2019, **58**, 14979-14985.

[S21] Y. Yuan, Q. Yu, J. Wen, C. Li, Z. Guo, X. Wang and N. Wang, *Angewandte Chemie International Edition*, 2019, **58**, 11785-11790.

[S22] C. Ma, J. Gao, D. Wang, Y. Yuan, J. Wen, B. Yan, S. Zhao, X. Zhao, Y. Sun, X. Wang and N. Wang, *Advanced Science*, 2019, **6**, 1900085.

[S23] J. Gao, Y. Yuan, Q. Yu, B. Yan, Y. Qian, J. Wen, C. Ma, S. Jiang, X. Wang and N. Wang, *Chemical Communications*, 2020, **56**, 3935-3938.

[S24] Z. Wang, Q. Meng, R. Ma, Z. Wang, Y. Yang, H. Sha, X. Ma, X. Ruan, X. Zou, Y. Yuan and G. Zhu, *Chem*, 2020, **6**, 1683-1691.

[S25] Y. Yuan, S. Zhao, J. Wen, D. Wang, X. Guo, L. Xu, X. Wang and N. Wang, *Advanced Functional Materials*, 2019, **29**, 1805380.

[S26] Y. H. Yuan, S. W. Feng, L. J. Feng, Q. H. Yu, T. T. Liu and N. Wang, *Angew. Chem.-Int. Edit.*, 2020, **59**, 4262-4268.

[S27] X. Xu, H. Zhang, J. Ao, L. Xu, X. Liu, X. Guo, J. Li, L. Zhang, Q. Li, X. Zhao, B. Ye, D. Wang, F. Shen and H. Ma, *Energy & Environmental Science*, 2019, **12**, 1979-1988.

[S28] Q. Yu, Y. Yuan, J. Wen, X. Zhao, S. Zhao, D. Wang, C. Li, X. Wang and N. Wang, *Advanced Science*, 2019, **6**, 1900002.

[S29] B. Yan, C. Ma, J. Gao, Y. Yuan and N. Wang, *Advanced Materials*, 2020, **32**, 1906615.

[S30] Y. Qian, Y. Yuan, H. Wang, H. Liu, J. Zhang, S. Shi, Z. Guo and N. Wang, *Journal of Materials Chemistry A*, 2018, **6**, 24676-24685.